

O.V. Marchuk¹, O.V. Smitiukh¹, Yu. Prots², A.O. Fedorchuk³

**Crystal Structure of Chalcogenides R'_xR''_yR'''_zPbSi₂S₈
(R' – La, R'' – Tb, R''' – Er)**

¹*Lesya Ukrainka Volyn National University, Lutsk, Ukraine, Marchuk.Oleg@vnu.edu.ua*

²*Max-Planck-Institut für Chemische Physik fester Stoffe, Dresden, Germany, prots@cpfs.mpg.de*

³*Stepan Gzhytskyi National University of Veterinary Medicine and Biotechnologies, Lviv, Ukraine, ft@ua.fm*

The La_xTb_yEr_zPbSi₂S₈ chalcogenides were obtained by synthesizing the elementary components in vacuum quartz containers at 1320 K. The synthesized alloys were homogenized by annealing at 770 K during 500 hours. The cell parameters of synthesized sulfides are: $a = 0.89576(3)$ nm, $c = 2.65646(8)$ nm – La_{1.2}Tb_{0.4}Er_{0.4}PbSi₂S₈; $a = 0.89209(1)$ nm, $c = 2.63466(5)$ nm – La_{0.9}Tb_{0.2}Er_{0.9}PbSi₂S₈; $a = 0.89002(3)$ nm, $c = 2.62714(7)$ nm – La_{0.67}Tb_{0.67}Er_{0.67}PbSi₂S₈; $a = 0.88993(1)$ nm, $c = 2.62973(4)$ nm – La_{0.6}Tb_{1.2}Er_{0.2}PbSi₂S₈; $a = 0.885161(7)$ nm, $c = 2.60445(3)$ nm – La_{0.2}Tb_{0.9}Er_{0.9}PbSi₂S₈ respectively.

The statistical mixture of (La, Tb, Er, Pb) atoms occupy 18e site (x y 1/4), and Si atoms occupy 12c site (1/3 2/3 z) in the structure of the obtained chalcogenides. Coordinating polyhedra of the statistical mixture (La, Tb, Er, Pb) atoms are trigonal prism with two additional atoms (CN = 8), and the Si atoms occupy the crystallographic point system 12c described with the tetrahedron. According to the experimental results, the synthesized chalcogenides crystallize in the La₂PbSi₂S₈ structure type (hR26,167). The structure of La₂PbSi₂S₈ is described by using the theory of second anion coordination (SAC).

Keywords: rare earth metals, crystal structure, powder X-ray diffraction, the closest coordination surrounding (CCS), the second coordination surrounding (SCS).

Received 11 June 2021; Accepted 15 October 2021.

Introduction

Search for new crystalline solids with tunable physical properties originating from the synergistic effect of the unique crystal structure and bonding nature is among the main streams in modern material science [1-3]. The properties and crystal structure of multi-component chalcogenides and rare earth metals (REM) containing chalcogenides [4-6], are investigated systematically regarding their practical utilization [7-12]. Adding REM atoms with different chemical nature in terms of 4f electronic level occupancy into the crystal structure of chalcogenides, is a good way to develop semiconductors with desired properties, as such examples are CaY₂Si₂S₈:Ce³⁺ [13], BaLa₂Si₂S₈:Eu²⁺ [14], (Gd,Ce)₄(SiS₄)₃, (Y,Ce)₄(SiS₄)₃ [15], (La,Ce,Y)₆Si₄S₁₇ [16], LaR'PbSi₂S₈, CeR'PbSi₂S₈, PrR'PbSi₂S₈ (R' = Ce, Pr, Sm, Tb, Dy, Y, Ho and Er) [17] and others. According to

the prospects of chalcogenide phases, which crystal structure consists of REM atoms, we can reasonably confirm that the synthesis of multi-component chalcogenides and detailed investigation of the relationship between their crystal structure and properties can be effectively utilized for designing new advanced functional materials.

In this work, we present results of investigations of crystal structures of chalcogenides La_{1.2}Tb_{0.4}Er_{0.4}PbSi₂S₈, La_{0.9}Tb_{0.2}Er_{0.9}PbSi₂S₈, La_{0.67}Tb_{0.67}Er_{0.67}PbSi₂S₈, La_{0.6}Tb_{1.2}Er_{0.2}PbSi₂S₈ and La_{0.2}Tb_{0.9}Er_{0.9}PbSi₂S₈, which are distinct compositions of the quasi-ternary La₂PbSi₂S₈ – Tb₂PbSi₂S₈ – Er₂PbSi₂S₈ system, by using of powder X-ray diffraction method.

I. Experimental section

Samples with stoichiometric compositions for investigation were prepared by co-melting high-purity elements in quartz containers evacuated to a residual pressure of 10^{-2} Pa. The total mass of the original batch for each sample was 1.0 g. The samples were synthesized in an MP-30 programmable electric muffle furnace by heating to 1370 K at the rate of 12 K/h, 2 h exposure, cooling to 770 K at 6 K/h. Homogenizing annealing at 770 K for 500 h was followed by quenching into room-temperature water without breaking the containers.

The crystal structure of sulfides $\text{La}_2\text{PbSi}_2\text{S}_8$, $\text{Tb}_2\text{PbSi}_2\text{S}_8$ and $\text{Er}_2\text{PbSi}_2\text{S}_8$ was detailedly investigated in work [18].

The result of calculations of unit cell of distinct compositions $\text{La}_{2-x}\text{Er}_x\text{PbSi}_2\text{S}_8$ and $\text{La}_{2-x}\text{Y}_x\text{PbSi}_2\text{S}_8$ of solid solution were presented in work [17].

The X-ray powder patterns of samples 1, 2, 4, 5, 9–13, 15, 16 and distinct compositions of $\text{Tb}_{2-x}\text{Er}_x\text{PbSi}_2\text{S}_8$ solid solution were obtained by using a DRON 4-13 powder diffractometer ($\text{CuK}\alpha$ radiation, $10^\circ \leq 2\Theta \leq 100^\circ$, step scan mode with a step size of 0.05°

and counting time of 20 s per data point). The unit cell parameters were calculated for these samples (Fig. 1 and Fig. 2).

The powder patterns of samples 3, 6, 7, 8 i 14 that corresponding to the compositions of $\text{La}_{1.2}\text{Tb}_{0.4}\text{Er}_{0.4}\text{PbSi}_2\text{S}_8$, $\text{La}_{0.9}\text{Tb}_{0.2}\text{Er}_{0.9}\text{PbSi}_2\text{S}_8$, $\text{La}_{0.67}\text{Tb}_{0.67}\text{Er}_{0.67}\text{PbSi}_2\text{S}_8$, $\text{La}_{0.6}\text{Tb}_{1.2}\text{Er}_{0.2}\text{PbSi}_2\text{S}_8$ and $\text{La}_{0.2}\text{Tb}_{0.9}\text{Er}_{0.9}\text{PbSi}_2\text{S}_8$ were obtained by using a Powder X-Huber Guinier Camera G670 ($\text{CuK}\alpha_1$ radiation, $\lambda = 1.54060 \text{ \AA}$, $3^\circ < 2\Theta < 100^\circ$, $\Delta 2\Theta = 0.005^\circ$, 6×30 min scans). The calculation of $\text{La}_{1.2}\text{Tb}_{0.4}\text{Er}_{0.4}\text{PbSi}_2\text{S}_8$, $\text{La}_{0.9}\text{Tb}_{0.2}\text{Er}_{0.9}\text{PbSi}_2\text{S}_8$, $\text{La}_{0.67}\text{Tb}_{0.67}\text{Er}_{0.67}\text{PbSi}_2\text{S}_8$, $\text{La}_{0.6}\text{Tb}_{1.2}\text{Er}_{0.2}\text{PbSi}_2\text{S}_8$ and $\text{La}_{0.2}\text{Tb}_{0.9}\text{Er}_{0.9}\text{PbSi}_2\text{S}_8$ crystal structure was performed by using Ritveld's method (program package WinCSD [19]). Visualization of the crystal structure was performed with VESTA program [20].

Results

The crystal structure of sulfides $\text{La}_{1.2}\text{Tb}_{0.4}\text{Er}_{0.4}\text{PbSi}_2\text{S}_8$, $\text{La}_{0.9}\text{Tb}_{0.2}\text{Er}_{0.9}\text{PbSi}_2\text{S}_8$, $\text{La}_{0.67}\text{Tb}_{0.67}\text{Er}_{0.67}\text{PbSi}_2\text{S}_8$, $\text{La}_{0.6}\text{Tb}_{1.2}\text{Er}_{0.2}\text{PbSi}_2\text{S}_8$ and

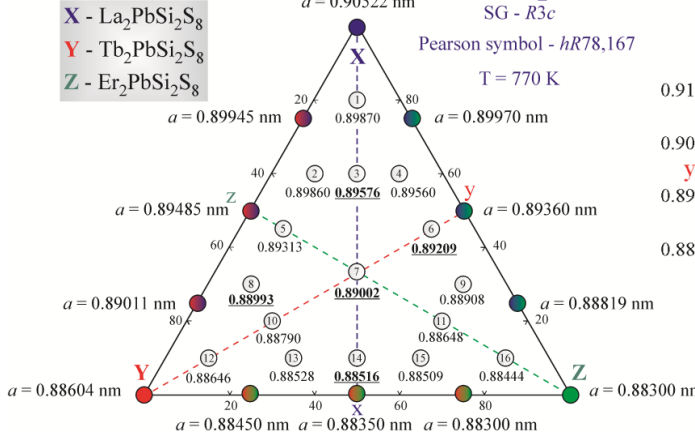
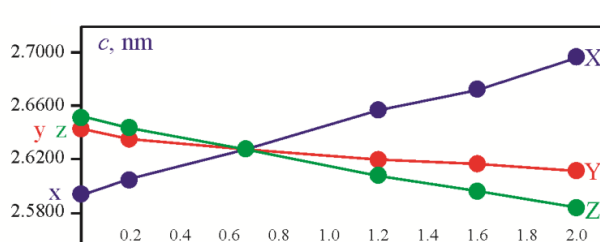
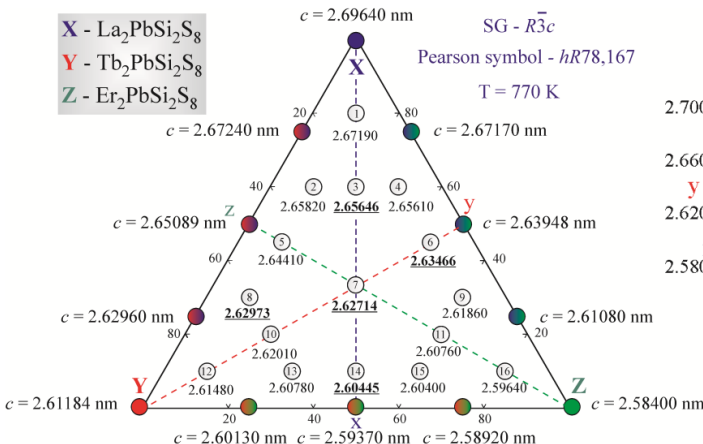
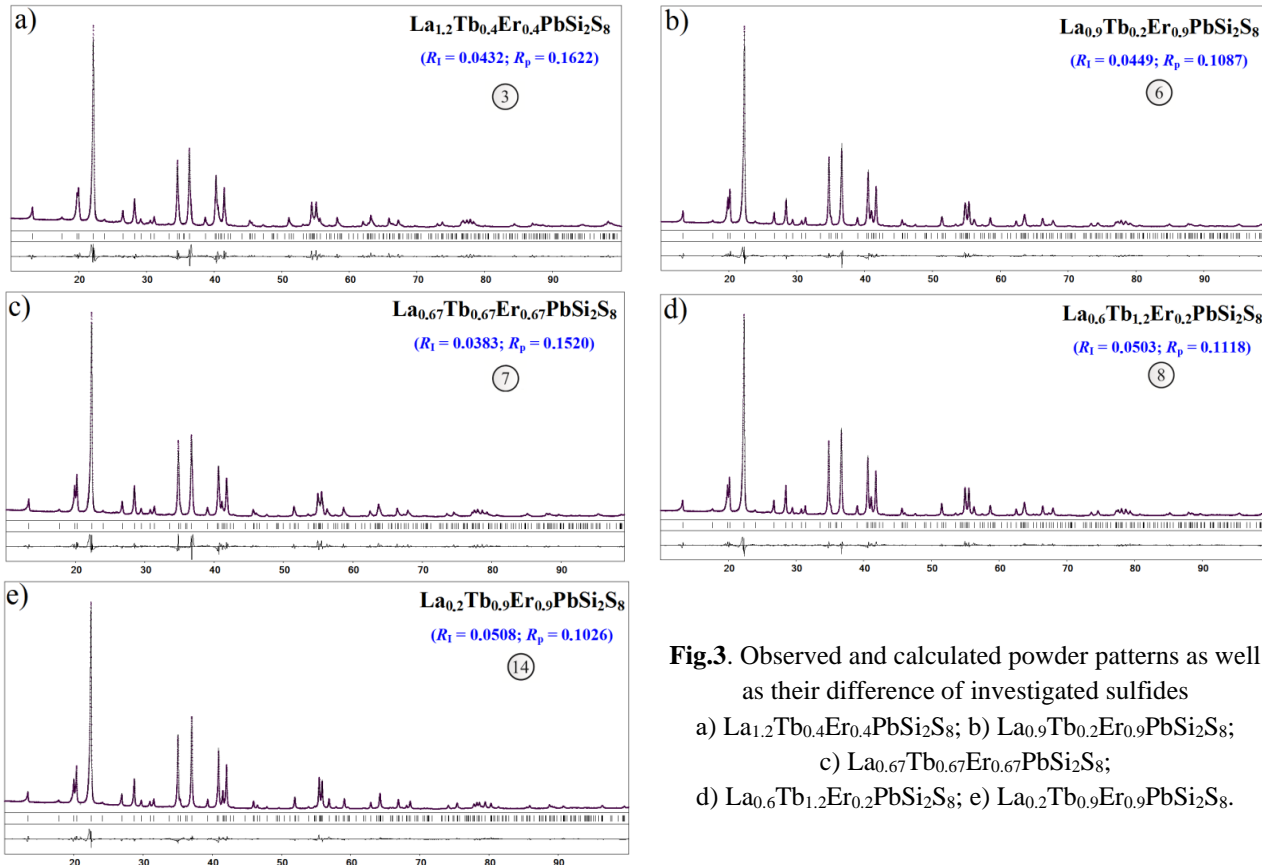


Fig. 1. Unit cell parameter a of sulfides $\text{La}_{2-m}\text{Tb}_m\text{PbSi}_2\text{S}_8$ ($m = 0; 0.5; 1.0; 1.5; 2.0$), $\text{La}_{2-n}\text{Er}_n\text{PbSi}_2\text{S}_8$ ($n = 0; 0.5; 1.0; 1.5; 2.0$), $\text{Tb}_{2-k}\text{Er}_k\text{PbSi}_2\text{S}_8$ ($k = 0; 0.5; 1.0; 1.5; 2.0$) and $\text{La}_x\text{Tb}_y\text{Er}_z\text{PbSi}_2\text{S}_8$.



Crystal Structure of Chalcogenides $R'_xR''_yR'''_zPbSi_2S_8$ ($R' - La$, $R'' - Tb$, $R''' - Er$)

$La_{0.2}Tb_{0.9}Er_{0.9}PbSi_2S_8$ was investigated by using powder X-ray diffraction method. The powder patterns of these chalcogenides (Fig. 3) were indexed in trigonal space group $R\bar{3}-c$.



Scan conditions and the results of the crystal structure refinement of obtained sulfides are presented in Tables 1 and 2. Analysis of hkl indexes and their intensities indicates that the crystal structure of obtained

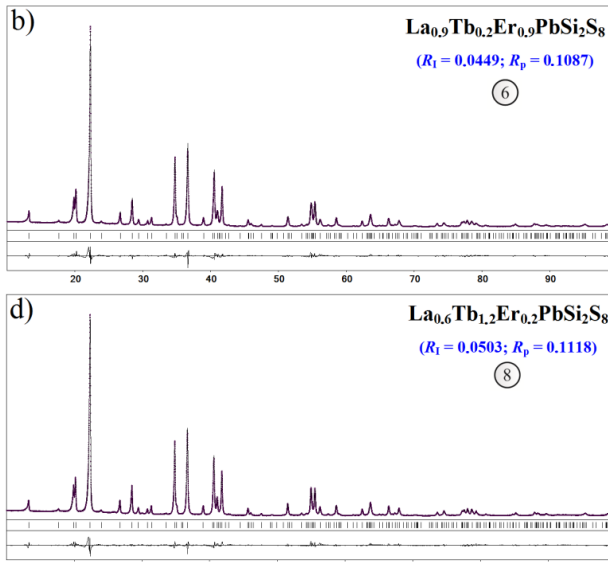


Fig.3. Observed and calculated powder patterns as well as their difference of investigated sulfides

- a) $La_{1.2}Tb_{0.4}Er_{0.4}PbSi_2S_8$; b) $La_{0.9}Tb_{0.2}Er_{0.9}PbSi_2S_8$;
- c) $La_{0.67}Tb_{0.67}Er_{0.67}PbSi_2S_8$;
- d) $La_{0.6}Tb_{1.2}Er_{0.2}PbSi_2S_8$; e) $La_{0.2}Tb_{0.9}Er_{0.9}PbSi_2S_8$.

Table 1

Scan conditions and the results of refinement of the crystal structure of obtained sulfides
 $La_{1.2}Tb_{0.4}Er_{0.4}PbSi_2S_8$ (A), $La_{0.9}Tb_{0.2}Er_{0.9}PbSi_2S_8$ (B) and $La_{0.67}Tb_{0.67}Er_{0.67}PbSi_2S_8$ (C)

Sulfide	A	B	C
a , (nm)	0.89576(3)	0.89209(1)	0.89002(3)
c , (nm)	2.65646(8)	2.63466(5)	2.62714(7)
V , (nm 3)	1.8459(2)	1.8158(8)	1.8022(1)
Number of atoms in cell	78	78	78
Calculated density (g/cm 3)	4.4585(4)	4.5325(2)	4.5666(3)
Absorption coefficient (1/cm)	777.79	790.69	796.64
2θ ; $\sin\theta/\lambda$ (max)	100.20; 0.498	99.56; 0.496	99.17; 0.494
R_I , R_p	0.0432; 0.1622	0.0449; 0.1087	0.0383; 0.1520
Scale factor	0.09792(0)	0.09834(0)	0.09738(0)

Table 2

Scan conditions and the results of refinement of the crystal structure of obtained sulfides
 $La_{0.6}Tb_{1.2}Er_{0.2}PbSi_2S_8$ (D) i $La_{0.2}Tb_{0.9}Er_{0.9}PbSi_2S_8$ (E)

Sulfide	D	E
a , (nm)	0.88993(1)	0.885161(7)
c , (nm)	2.62973(4)	2.60445(3)
V , (nm 3)	1.80364(8)	1.76722(5)
Number of atoms in cell	78	78
Calculated density (g/cm 3)	4.5170(2)	4.7699(2)
Absorption coefficient (1/cm)	939.09	817.76
2θ ; $\sin\theta/\lambda$ (max)	99.87; 0.497	100.20; 0.498
R_I , R_p	0.0503; 0.1118	0.0508; 0.1026
Scale factor	0.09706(0)	0.09789(0)

chalcogenides belongs to the structure type $\text{La}_2\text{PbSi}_2\text{S}_8$ (*hR26,167*).

Refinement of atomic coordinates and isotropic thermal parameters (Table 3) in the model satisfies the value of the discrepancy factor.

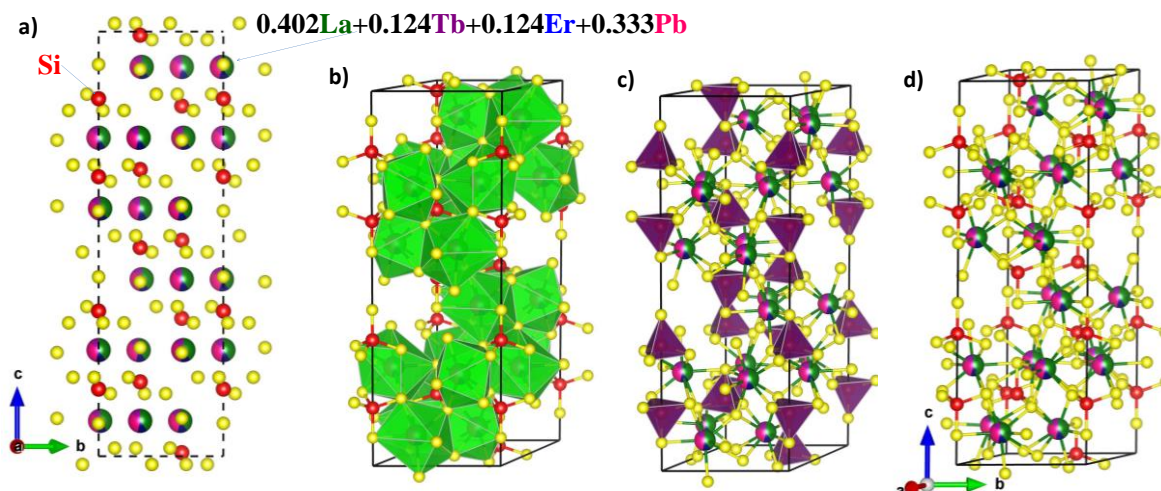
In the structure of chalcogenides $\text{La}_x\text{Tb}_y\text{Er}_z\text{PbSi}_2\text{S}_8$, atoms of statistical mixture M1, M2, M3, M4 i M5 are located at the site – $18e$. The statistical mixture are of the

following composition: M1 – 41 % La 13 % Tb, 13 % Er, 33 % Pb, M2 – 30 % La, 7 % Tb, 30 % Er, 33 % Pb, M3 – 22 % La, 22 % Tb, 22 % Er, 33 % Pb, M4 – 20 % La, 40 % Tb, 7 % Er, 33 % Pb i M5 – 7 % La, 30 % Tb, 30 % Er, 33 % Pb. Atoms of Si occupy the site $12c$, and atoms of Sulfur occupy two sites $12c$ and $36f$ (Fig. 4a). Atoms of statistical mixture M(1-5) coordinate around themselves eight atoms of S, forming trigonal prisms with

Table 3

Atomic coordinates and anisotropic thermal parameters of $\text{La}_x\text{Tb}_y\text{Er}_z\text{PbSi}_2\text{S}_8$

Atom	Site	<i>x</i>	<i>y</i>	<i>z</i>	$B_{130} \times 10^{-2}$ (nm ²)
$\text{La}_{1.2}\text{Tb}_{0.4}\text{Er}_{0.4}\text{PbSi}_2\text{S}_8$					
M1	$18e$	0.3200(1)	0.3200(1)	1/4	2.40(2)
Si	$12c$	1/3	2/3	0.3245(3)	2.40(2)
S1	$12c$	1/3	2/3	0.2454(3)	2.40(2)
S2	$36f$	0.0351(5)	0.2380(4)	0.1860(2)	2.40(2)
$\text{La}_{0.9}\text{Tb}_{0.2}\text{Er}_{0.9}\text{PbSi}_2\text{S}_8$					
M2	$18e$	0.32097(9)	0.32097(9)	1/4	2.69(2)
Si	$12c$	1/3	2/3	0.3238(2)	2.69(2)
S1	$12c$	1/3	2/3	0.2447(2)	2.69(2)
S2	$36f$	0.0350(4)	0.2389(3)	0.18664(9)	2.69(2)
$\text{La}_{0.67}\text{Tb}_{0.67}\text{Er}_{0.67}\text{PbSi}_2\text{S}_8$					
M3	$18e$	0.3214(1)	0.3214(1)	1/4	2.53(2)
Si	$12c$	1/3	2/3	0.3238(3)	2.53(2)
S1	$12c$	1/3	2/3	0.2435(2)	2.53(2)
S2	$36f$	0.0354(4)	0.2416(3)	0.1873(1)	2.53(2)
$\text{La}_{0.6}\text{Tb}_{1.2}\text{Er}_{0.2}\text{PbSi}_2\text{S}_8$					
M4	$18e$	0.32098(9)	0.32098(9)	1/4	2.83(2)
Si	$12c$	1/3	2/3	0.3248(2)	2.83(2)
S1	$12c$	1/3	2/3	0.2442(2)	2.83(2)
S2	$36f$	0.0353(4)	0.2397(3)	0.18587(9)	2.83(2)
$\text{La}_{0.2}\text{Tb}_{0.9}\text{Er}_{0.9}\text{PbSi}_2\text{S}_8$					
M5	$18e$	0.32169(7)	0.32169(7)	1/4	3.00(1)
Si	$12c$	1/3	2/3	0.3252(2)	3.00(1)
S1	$12c$	1/3	2/3	0.2434(2)	3.00(1)
S2	$36f$	0.0357(3)	0.2420(3)	0.18706(7)	3.00(1)

**Fig. 4.** Unit cell and the coordination polyhedra of the $\text{La}_x\text{Tb}_y\text{Er}_z\text{PbSi}_2\text{S}_8$ chalcogenides structure.

two additional atoms [$M(1-5) 6S_2 2S_1$] (Fig. 4b), and atoms of Silicon, occupying the site $12c$, have tetrahedral surrounding [$Si 1S_1 3S_2$] (Fig. 4c). 3D-model of the unit cell in the structure of the above-described chalcogenides are presented in Figure 4d.

The inter-atomic distances $\delta(M1 - S)$, $\delta(M2 - S)$, $\delta(M3 - S)$, $\delta(M4 - S)$, $\delta(M5 - S)$, $\delta(Si - S)$ and coordination numbers in the structure of $La_xTb_yEr_zPbSi_2S_8$ compound are presented in Tables 4-6.

It is worth noticing of regular change of inter-atomic distances $\delta(M-S)$ of the structure of chalcogenides $La_{0.2}Tb_{0.9}Er_{0.9}PbSi_2S_8$, $La_{0.67}Tb_{0.67}Er_{0.67}PbSi_2S_8$, $La_{1.2}Tb_{0.4}Er_{0.4}PbSi_2S_8$ and $La_2PbSi_2S_8$, in which stoichiometric composition is on the height xX of Gibbs-Roozeboom's triangular (Fig. 1 and Fig. 2).

With an increase in the content of La ($r(La^{3+}) = 0.130$ nm, [21]) and, accordingly, a decrease in the content of Tb ($r(Tb^{3+}) = 0.118$ nm) and Er ($r(Er^{3+}) = 0.114$ nm) in the site $18e$ there is a regular

increase interatomic distances $\delta(M-S)_{min}$ from 0.2794 to 0.2880 nm; interatomic distances $\delta(M-S)_{max}$ increase from 0.3241 to 0.3278 nm (Fig. 5).

For the heights yY and zZ , it is regularly to expect a reduction of inter-atomic distances $\delta(M-S)$ since the contents of REM, which has lower ionic radii, is growing at site $18e$. These patterns correlate well with the change in the parameters a and c of the unit cell of sulfides, the stoichiometric composition of which falls at the heights xX , yY and zZ of the Gibbs-Rooseboom triangle (Fig. 1 and Fig. 2).

II. Discussion of results

The compounds, in which structure cations of heavy atoms are located within the anionic sublattice of light atoms, can reveal interesting physical properties [22, 23].

Table 4

The inter-atomic distances δ (nm) and coordination numbers (CN) of the atoms of the structure $La_xTb_yEr_zPbSi_2S_8$

Atoms			δ , nm	CN	Atoms			δ , nm	CN	
$La_{1.2}Tb_{0.4}Er_{0.4}PbSi_2S_8$					$La_{0.9}Tb_{0.2}Er_{0.9}PbSi_2S_8$					
M1	-2S2	0,2840(4)	8	M2	-2S2	0,2822(3)	8	M2	-2S2	0,2941(3)
	-2S2	0,2955(4)			-2S2	0,30335(8)			-2S1	0,30335(8)
	-2S1	0,3050(1)			-2S2	0,3263(3)			-2S2	0,3282(4)
	-2S2	0,3282(4)			-1S1	0,2085(7)			-3S2	0,2139(3)
Si	-1S1	0,2099(11)	4	Si	-1S1	0,2120(8)	4	Si	-3S2	0,2163(4)
	-3S2	0,2129(5)			-3S2	0,2124(3)				

Table 5

The inter-atomic distances δ (nm) and coordination numbers (CN) of the atoms of the structure $La_xTb_yEr_zPbSi_2S_8$

Atoms			δ , nm	CN	Atoms			δ , nm	CN	
$La_{0.67}Tb_{0.67}Er_{0.67}PbSi_2S_8$					$La_{0.6}Tb_{1.2}Er_{0.2}PbSi_2S_8$					
M3	-2S2	0.2808(3)	8	M4	-2S2	0.2827(3)	8	M4	-2S2	0.2915(3)
	-2S2	0.2942(3)			-2S1	0.30268(9)			-2S1	0.30268(9)
	-2S1	0.3026(1)			-2S2	0.3269(3)			-2S2	0.3254(3)
	-2S2	0.3254(3)			-1S1	0.2120(8)			-3S2	0.2109(8)
Si	-1S1	0.2109(8)	4	Si	-1S1	0.2124(3)		Si	-3S2	0.2163(4)
	-3S2	0.2163(4)			-3S2	0.2124(3)				

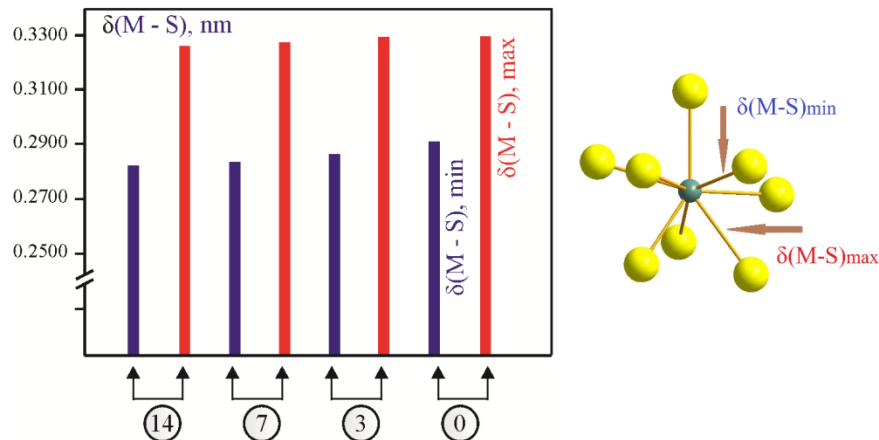


Fig. 5. The inter-atomic distances $\delta(M-S)$ of the structure of sulfides $La_xTb_yEr_zPbSi_2S_8$: 14 – $La_0.2Tb_{0.9}Er_{0.9}PbSi_2S_8$; 7 – $La_{0.67}Tb_{0.67}Er_{0.67}PbSi_2S_8$; 3 – $La_{1.2}Tb_{0.4}Er_{0.4}PbSi_2S_8$ and 0 – $La_2PbSi_2S_8$.

Table 6

The inter-atomic distances δ (nm) and coordination numbers (CN) of the atoms of the structure $\text{La}_{0.2}\text{Tb}_{0.9}\text{Er}_{0.9}\text{PbSi}_2\text{S}_8$

Atoms	δ , nm	CN
M5	- 2S2 0.2794(2)	8
	- 2S2 0.2910(2)	
	- 2S1 0.30084(7)	
	- 2S2 0.3241(2)	
Si	- 1S1 0.2130(6)	4
	- 3S2 0.2137(3)	

The probability of formation of new compounds increases in the systems where initial components are different significantly with their chemical and physical properties, as an example of such is a quasi-ternary $\text{La}_2\text{S}_3 - \text{PbS} - \text{SiS}_2$ system (Fig. 6), in which exists the quaternary $\text{La}_2\text{PbSi}_2\text{S}_8$ compound, which crystallizes in its own structure type (*hR26.167* [8]). The crystal structure of obtained chalcogenides belongs to the structure type $\text{La}_2\text{PbSi}_2\text{S}_8$. The ternary sulfide La_2PbS_4 , La_2SiS_5 i Pb_2SiS_4 compounds exist in the quasi-binary $\text{La}_2\text{S}_3 - \text{PbS}$, $\text{La}_2\text{S}_3 - \text{SiS}_2$ and $\text{PbS} - \text{SiS}_2$ systems, respectively.

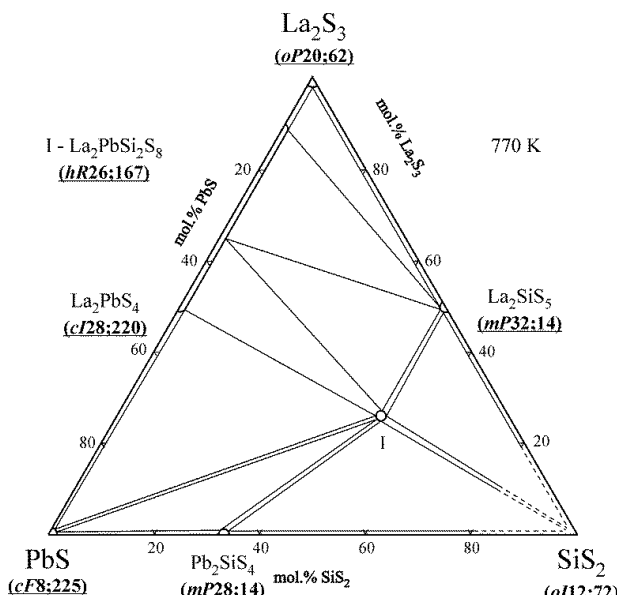


Fig. 6. The quasi-ternary $\text{La}_2\text{S}_3 - \text{PbS} - \text{SiS}_2$ system at the 770 K.

In the structure of the PbS and SiS_2 compounds, the second coordination surrounding (SCS) of anionic atoms has a form of the cuboctahedron, and such a situation indicates the predominant component of the ionic type of interaction, and asymmetric SCS of the La_2S_3 structure indicates the significantly covalent component.

In the PbS structure (*cF8.225* [24]), atoms of Lead are located in the octahedral cavities of the SCS; and in the structure of SiS_2 (*oI12.72*) [25]), atoms of Silicon are located in the tetrahedral cavities of the SCS (Fig. 7). In other words, a bigger atom occupies bigger cavities; fewer atoms occupy less ones where in the nodes of the anionic sublattice are sulfur atoms. The dense

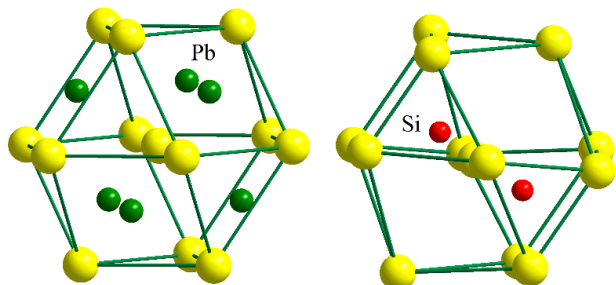


Fig. 7. SCS of atoms of Sulfur of the structure PbS (*cF8.225*) and SiS_2 (*oI12.72*).

arrangement of atoms and the large difference in the electronegativities of the sulfur atoms and the *p*-elements of the sixth group indicate the ionic type of bond in the PbS and SiS_2 compounds.

In the structure of La_2S_3 (*oP20.62* [26.27]), atoms of Lanthanum are located in the trigonal prisms with two additional atoms of Sulfur against the side faces. Such a surrounding testifies that despite the big difference of electronegativity of atoms La and S, the dense arrangement of atoms is not observed.

In the process of interactions between sulfides of Pb and Si comes to existence Pb_2SiS_4 compound (*mP28.14* [28]), in which structure the anionic type of sublattice are saved, that is why as in the original sulfides it looks like the cuboctahedron (Fig. 8).

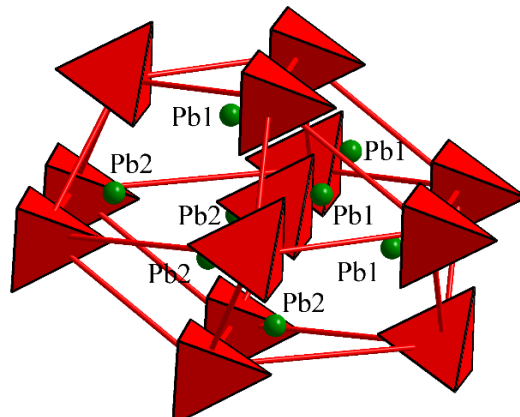


Fig. 8. SCS of atoms anionic group $[\text{SiS}_4]^{4-}$ of the structure of Pb_2SiS_4 compound (*mP28.14*).

Due to the interaction of sulfides of two competing *p*-elements, more electronegative Silicon forms the tetrahedral surrounding, and these tetrahedra are considered like anions, and less electronegative Lead occupies the cation site. In this case, it can be argued that there are tetrahedra $[\text{SiS}_4]$ in the anionic sublattice nodes, and as a result, the atoms of Lead will occupy smaller cavities within the SCS – tetrahedra of anion atoms. The closest coordination surrounding (CCS) of the atoms of Lead are trigonal prisms of sulfur atoms. Due to the fact that the anions have become larger, and the atoms of Pb occupy a favorable position for them, we have the preservation of the anionic sublattice and Silicon becomes an anion-forming element.

From the point of view of the structure and the properties of sulfides, which have pronounced ionic

properties, it is interesting to introduce into their structure rare earth elements, which in the structure of binary sulfides form covalent bonds $R - S$. In the structure of binary sulfides, REM atoms form the closest surrounding, which is not characteristic of dense stacking (these are usually trigonal prisms with additional atoms). REM atoms do not form ionic structures, but when they are incorporated into an ionic structure, it is possible to form crystal structures where dense packages are formed. An example of such a structure is La_2SiS_5 (*mP32.14* [29]) where $Si_2S_8^{8-}$ ions are located in the anionic sublattice nodes. Atoms of the cationic group in the form of tetrahedra of lanthanum atoms around sulfur atoms are located in tetrahedral cavities within the SCS. The polyhedra of the cationic group are connected by edges and vertices. The CCS of Lanthanum atoms has the form of trigonal prisms with two (for La1) and three (for La2) additional atoms against the side faces.

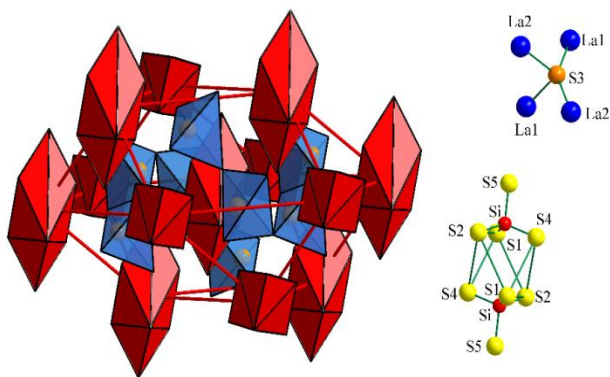


Fig. 9. SCS of atoms of the anionic group $[Si_2S_8^{8-}]$ of the structure of La_2SiS_5 (*mP32.14*).

In the crystal structure of La_2PbS_4 (*cI28.220* [30]), the formation of trigonal prisms with two additional sulfur atoms is characteristic for Lanthanum atoms. In the structure of the La_2PbS_4 compound, SCS of Sulfur atoms in the form of asymmetric polyhedra with eleven atoms indicates a significant covalent component in the bonds, and therefore to emit ions and cations incorrectly. Hence, the quasi-ternary $La_2S_3 - PbS - SiS_2$ system is unique since the crystal structure of the part of the original phases can be described by SCS in the form of the cuboctahedron. However, adding REM creates a platform for the emergence of non-standard structural fragments. This leads to the fact that the crystal structure of La_2PbSiS_8 (*hR26.167*) can also be considered as dense ion stacking. The SCS of the compound is in the form of the cuboctahedron (Fig. 10) where $Si_2S_8^{8-}$ ions are located in the anionic sublattice nodes of La_2SiS_5 . The cationic atoms are located at the boundary of tetrahedral and octahedral cavities within SCS and have CCS in the form of trigonal prisms of sulfur atoms.

The analysis of the La_2PbSiS_8 crystal structure indicates its prospect as a nonlinear optical material. The peculiarity of the structure of La_2PbSiS_8 is that the

positions of Lanthanum can be purposefully replaced by different atoms of REM, which greatly expands the possibilities for the synthesis of new compounds with promising properties.

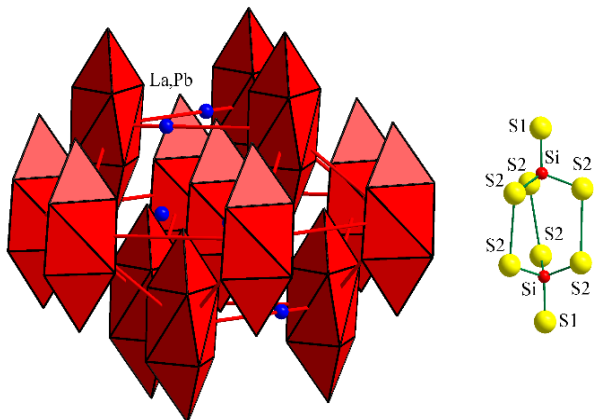


Рис. 10. ДКО атомів аніонної групи у структурі сполуки La_2PbSiS_8 (*hR26.167*).

Conclusions

In this work, we present the results of the crystal structure investigation of complex chalcogenide phases $La_{1.2}Tb_{0.4}Er_{0.4}PbSi_2S_8$, $La_{0.9}Tb_{0.2}Er_{0.9}PbSi_2S_8$, $La_{0.67}Tb_{0.67}Er_{0.67}PbSi_2S_8$, $La_{0.6}Tb_{1.2}Er_{0.2}PbSi_2S_8$ and $La_{0.2}Tb_{0.9}Er_{0.9}PbSi_2S_8$ which are the distinct compositions of continuous solid solutions of the quasi-ternary $La_2PbSi_2S_8 - Tb_2PbSi_2S_8 - Er_2PbSi_2S_8$ system. These phases are obtained by populating the site $18e$ ($x\ y\ 1/4$) with atoms of different REM. Their crystal structure belongs to the structural type La_2PbSiS_8 (*hR26.167*).

The crystal structure of the La_2PbSiS_8 compound from the standpoint of the theory of SCS is described for the first time. The crystal structure of the La_2PbSiS_8 is unique because the part of this structure can be described through the second coordination surrounding. However, another part, which includes La atoms cannot be described through the second coordination surrounding because of the big coordination number of atoms La. Thereby, the compound has more ionic bonds than covalent ones. Such types of bonds indicate the high possibility of good optical properties of the studied compounds.

Marchuk O.V. - PhD., Associate Professor, Associate Professor of Chemistry and Technology;
Smitiukh O.V. - PhD., senior laboratory assistant of the Department of Chemistry and Technology;
Prots Yu. - Ph.D., Co-worker of the Department of Chemical Metals Science;
Fedorchuk A.O. - Doctor of Technical Sciences, Professor, Professor of the Department of Biological and General Chemistry.

[1] G. Tan, L. D. Zhao, M. G. Kanatzidis, <https://doi.org/10.1021/acs.chemrev.6b00255>.

Chem. Rev. 116, 12123 (2016);

- [2] X. L. Shi, J. Zou, Z. G. Chen, Chem. Rev. 120, 7399 (2020); <https://doi.org/10.1021/acs.chemrev.0c00026>.
- [3] C. Celania, A.-V. Mudring, J. Solid State Chem. 274, 243 (2019); <https://doi.org/10.1016/j.jssc.2019.03.009>.
- [4] T. Parashchuk, I. Horichok, A. Kosonowski, O. Cherniushok, P. Wyzga, G. Cempura, A. Kruk, K. Wojciechowski, J. Alloys Compd. 860, 158355 (2021); <https://doi.org/10.1016/j.jallcom.2020.158355>.
- [5] A.O. Fedorchuk, O.V. Parasyuk, O. Cherniushok, B. Andriyevsky, G.L. Myronchuk, O.Y. Khyzhun, G. Lakshminarayana, J. Jedryka, I.V. Kityk, A.M. EINagar, A.A. Albassam, M. Piasecki, J. Alloys Compd. 740, 294 (2018); <https://doi.org/10.1016/j.jallcom.2017.12.353>.
- [6] O. Cherniushok, R. Cardoso-Gil, T. Parashchuk, Y. Grin, K. T. Wojciechowski, Inorg. Chem. 60, 2771 (2021); <https://doi.org/10.1021/acs.inorgchem.0c03549>.
- [7] M. Daszkiewicz, L.D. Gulay, V.Ya. Shemet, Acta Cryst. B. 64(2), 172 (2008); <https://doi.org/10.1107/S0108768108004175>.
- [8] L.D. Gulay, M. Daszkiewicz, I.P. Ruda, O.V. Marchuk, Acta Cryst. C. 66(3), i19 (2010); <https://doi.org/10.1107/S0108270110000247>.
- [9] H-Y. Zeng, F-K. Zheng, G-C. Guo, J-S. Huang, J. Alloys Compd. 458, 123 (2008); <https://doi.org/10.1016/j.jallcom.2007.03.136>.
- [10] Y. Nanai, C. Sasaki, Yu Sakamoto, T. Okuno, J. Phys. D: Appl. Phys. 44, 405402 (2011); <https://doi.org/10.1088/0022-3727/44/40/405402>.
- [11] A. Choudhury, P.K. Dorhout, Z. Anorg. Allg. Chem. 634, 649 (2008); <https://doi.org/10.1002/zaac.200700511>.
- [12] Y. Nanai, Y. Suzuki, T. Okuno, J. Phys. D: Appl. Phys. 49, 105103 (2016); <https://doi.org/10.1088/0022-3727/49/10/105103>.
- [13] S.P. Lee, C.H. Huang, T.M. Chen, J. Mater. Chem. C. 2(42), 8925 (2014); <https://doi.org/10.1039/c4tc01572j>.
- [14] S.P. Lee, T.S. Chan, T.M. Chen, ACS Appl. Mater. Interfaces. 7(1), 40 (2015); <https://doi.org/10.1021/am505613s>.
- [15] Y. Nanai, K. Suzuki, T. Okuno, Mater. Res. Express. 2, 036203 (2015); <https://doi.org/10.1088/2053-1591/2/3/036203>.
- [16] Y. Nanai, H. Kamioka, T. Okuno, J. Phys. D Appl. Phys. 51, 135103 (2018); <https://doi.org/10.1088/1361-6463/aaaf5e>.
- [17] D. Kaczorowski, Kh.O. Melnychuk, O.V. Marchuk, L.D. Gulay, M. Daszkiewicz, J. Solid State Chem. 290, 121565 (2020); <https://doi.org/10.1016/j.jssc.2020.121565>.
- [18] M. Daszkiewicz, O.V. Marchuk, L.D. Gulay, D. Kaczorowski, J. Alloys compd. 519, 85 (2012); <https://doi.org/10.1016/j.jallcom.2011.12.097>.
- [19] L. Akselrud, Yu. Grin. J. Appl. Cryst. 47, 803 (2014); <https://doi.org/10.1107/S1600576714001058>.
- [20] K. Momma, F. Izumi, J. Appl. Crystallogr. 44, 1272 (2011); <https://doi.org/10.1107/S0021889811038970>.
- [21] R.D. Shannon, Acta Cryst. A. 39, 751 (1976); <https://doi.org/10.1107/S0567739476001551>.
- [22] R. Ahiska, D. Freik, T. Parashchuk, I. Gorichok, Turk. J. Phys. 38(1), 125 (2014); <https://doi.org/10.3906/fiz-1301-7>.
- [23] I.V. Horichok, L.I. Nykyruy, T.O. Parashchuk, S.D. Bardashevskaya and M.A. Pylyponuk, Mod. Phys. Lett. B 30, 1650172 (2016); <https://doi.org/10.1142/S0217984916501724>.
- [24] T.K. Chattopadhyay, H.G. von Schnering, W. Grosshans, W.B. Holzapfel, Physica B + C. 139, 356 (1986); [https://doi.org/10.1016/0378-4363\(86\)90598-X](https://doi.org/10.1016/0378-4363(86)90598-X).
- [25] J. Peters, B. Krebs, Acta Cryst. 38, 1270 (1982); <https://doi.org/10.1107/S0567740882005469>.
- [26] P. Basançon, C. Adolphe, J. Flahaut, P. Laruelle, Mat. Res. Bull. 4, 227 (1969); [https://doi.org/10.1016/0025-5408\(69\)90098-1](https://doi.org/10.1016/0025-5408(69)90098-1).
- [27] W.H. Zachariasen, Acta Cryst. 1, 265 (1948); <https://doi.org/10.1107/S0365110X48000703>.
- [28] J.E. Iglesias, H. Steinfink, J. Solid State Chem. 6(1), 93 (1973); [https://doi.org/10.1016/0022-4596\(73\)90209-0](https://doi.org/10.1016/0022-4596(73)90209-0).
- [29] A. Michelet, G. Perez, J. Etienne, M. Darriet-Duale, C. R. Acad. Sci. 271, 513 (1970).
- [30] M. Patrie, M. Guittard, M. P. Pardo, Mat. Res. Bull. 11, 3832 (1969).

О.В. Марчук¹, О.В. Смітюх¹, Ю. Проць², А.О. Федорчук³

Кристалічна структура халькогенідів $R'_xR''_yR'''_zPbSi_2S_8$ ($R' - La$, $R'' - Tb$, $R''' - Er$)

¹Волинський національний університет імені Лесі Українки, Луцьк, Україна, Marchuk.Oleg@vnu.edu.ua

²Інститут хімічної фізики твердого тіла Товариства Макса Планка, Дрезден, Німеччина, prots@cpfs.mpg.de

³Львівський національний університет ветеринарної медицини та біотехнологій імені С.З. Гжицького, Львів, Україна, ft@ua.fm

Халькогеніди, загального компонування $La_xTb_yEr_zPbSi_2S_8$, отримували методом спікання елементарних компонентів у вакуумованих кварцевих контейнерах за температури 1320 К. Синтезовані сплави гомогенізували відпалом за температури 770 К протягом 500 год. Розраховано параметри елементарної комірки: $a = 0,89576(3)$ нм, $c = 2,65646(8)$ нм для сульфіду $La_{1,2}Tb_{0,4}Er_{0,4}PbSi_2S_8$; $a = 0,89209(1)$ нм, $c = 2,63466(5)$ нм для сульфіду $La_{0,9}Tb_{0,2}Er_{0,9}PbSi_2S_8$; $a = 0,89002(3)$ нм, $c = 2,62714(7)$ нм для сульфіду $La_{0,67}Tb_{0,67}Er_{0,67}PbSi_2S_8$; $a = 0,88993(1)$ нм, $c = 2,62973(4)$ нм для сульфіду $La_{0,6}Tb_{1,2}Er_{0,2}PbSi_2S_8$; $a = 0,885161(7)$ нм, $c = 2,60445(3)$ нм для сульфіду $La_{0,2}Tb_{0,9}Er_{0,9}PbSi_2S_8$. У структурі синтезованих халькогенідів атоми статистичної суміші (La, Tb, Er, Pb) займають положення $18e$ (х у 1/4), атоми Si займають положення $12c$ (1/3 2/3 z). Координатними многогранниками для атомів статистичної суміші (La, Tb, Er, Pb) є призми з двома додатковими атомами (КЧ = 8), а атоми Si, займаючи ПСТ $12c$, мають тетраедричне оточення з атомів Сульфуру. Результати експерименту підтвердили, що синтезовані халькогеніди кристалізуються у структурному типі $La_2PbSi_2S_8$ ($hR26,167$). Структуру $La_2PbSi_2S_8$ описано з позицій теорії ДКО.

Ключові слова: рідкісноземельні метали, кристалічна структура, рентгенівський метод порошку, найближче координаційне оточення (НКО), друге координаційне оточення (ДКО).